Environ. Sci. Technol. **1999**, *33,* 635−641

Analysis of Air Quality Data Using Positive Matrix Factorization

KURTIS G. PATERSON,*
JESSICA L. SAGADY, AND
DIANNE L. HOOPER
Department of Civil and Environmental Engineering, Michigan Technological University, Houghton, Michigan 49931

STEVE B. BERTMAN
Department of Chemistry, Western Michigan University, Kalamazoo, Michigan 49008

MARY ANNE CARROLL
Department of Atmospheric, Oceanic, and Space Sciences, University of Michigan, Ann Arbor, Michigan 48109

PAUL B. SHEPSON
Departments of Chemistry and Earth and Atmospheric Sciences, Purdue University, West Lafayette, Indiana 47907

Positive matrix factorization (PMF) was applied to air quality and temperature data collected as part of the Program for Research on Oxidants: Photochemistry, Emissions, and Transport 1997 summer measurement campaign. Unlike more conventional methods of factor analysis such as principal component analysis, PMF produces non-negative factors, aiding factor interpretation, and utilizes error estimates of the data matrix. This work uses PMF as a means of source identification and apportionment, important steps in the development of air pollution control strategies. Measurements of carbon monoxide, particulate matter, peroxyactyl nitrate (PAN), isoprene, temperature, and ozone were taken from a 31 m tower in rural northern Michigan and analyzed in this study. PMF resulted in three physically interpretable factors: an isoprene-dominated factor, a local source factor, and a long-range transport factor. The isoprene-dominated and local source factors exhibited strong and weak diurnal signals, respectively. Factor strengths for the long-range transport factor were relatively high during periods of south and southwesterly flow. The average contribution of the three factors was determined for each pollutant, enabling the modeled matrix to be compared to the data matrix. Good agreement between the fitted and data matrix was achieved for all parameters with the exception of coarse particulate matter. The PMF model explained at least 75% of variation for all species analyzed.

Introduction

Identification of air pollution source characteristics is an important step in the development of regional air quality control strategies. Receptor modeling, using measurements of pollutant concentrations at one or more sample sites, is often a reliable way to provide information regarding source regions of air pollution (*1*). One such receptor modeling technique is principal component analysis (PCA), a special case of factor analysis (*2*). PCA has long been applied as a tool for source identification in air quality studies (*3*−*9*). However, Paatero and Tapper (*10*) have argued that a new variant of factor analysis, positive matrix factorization (PMF), is better suited to environmental applications than PCA. Unlike PCA, PMF utilizes the known (or estimated) errors of the data matrix and imposes non-negativity constraints on the resulting factors. Successful implementation of PMF has been reported in source identification studies of precipitation samples (*11, 12*).

To determine the applicability of this new type of factor analysis as a source identification tool for atmospheric pollutants, PMF was performed on air quality and meteorological measurements made during the 1997 Program for Research on Oxidants: PHotochemistry, Emissions, and Transport (PROPHET) summer measurement campaign. The broad goal of PROPHET was to investigate the production and transport of ozone and its precursors to a rural, boundary layer site in the Midwest. More specific objectives included seasonal ozone characterization, a determination of the roles of anthropogenic and biogenic hydrocarbon emissions in ozone production, and source identification, as will be discussed in this paper. To meet these objectives, coordinated measurements of atmospheric particulate matter, gaseous constituents, and meteorology were made at a rural field site near the northern tip of Michigan's lower peninsula.

The Experimental Section of this paper presents the atmospheric data, PMF method, and transport modeling used in this study. The Results section describes the findings from these analyses.

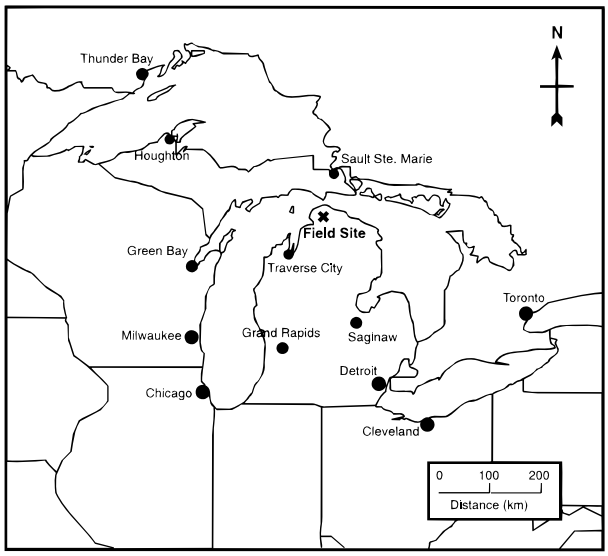

FIGURE 1. Regional map surrounding the field measurement site. Location of the measurement site (84° 42′ 53″ W, 45° 33′ 34″ N) is presented with respect to several cities and denoted with an X.

Experimental Section

Data. All measurements were taken from atop a 31.4 m tower located in a forested region approximately 10 km east of the small town of Pellston, MI (84° 42′ 53″ W, 45° 33′ 34″ N, elevation 234.1 m above mean sea level). Figure 1 presents a regional map of the study domain. Interstate-75 runs north−south 9 km east of the tower site, and a small regional airport is located in Pellston. The rural area surrounding the tower

* Corresponding author telephone: (906) 487-3495; fax: (906) 487-2943; e-mail address: paterson@mtu.edu.

10.1021/es980605j CCC: $18.00
Published on Web 02/15/1999

TABLE 1. Parameters Measured during the PROPHET 1997 Summer Measurement Campaign, Methods of Measurement, and Measurement Times

parameter	method of measurement	measurement time
isoprene	automated solid sorbent preconcentrator/GC/MS system, as described in Starn et al. (*13*)	2−4 min samples taken on the hour, 20 min after the hour, or 20 min before the hour
carbon monoxide (CO)	Thermo Environmental Instrument Model 48C trace level CO analyzer−gas filter correlation, nondispersive IR absorption	1-min averages
peroxyacetyl nitrate (PAN)	CG with electron capture detector and whole air injection, as described in Nouaime et al. (*14*)	1-min samples taken every 20 min
particulate matter (PM), coarse (diameter > 1.5 μm)	Particulate Measuring Systems Model LAS-X-laser aerosol spectrometer	10-s sampling time—entire range recorded every 40 s
particulate matter (PM), fine (0.12 μm < diameter < 1.5 μm)	Particulate Measuring Systems Model LAS-X-laser aerosol spectrometer	10-s sampling time—entire range recorded every 40 s
ozone	Thermo Environmental Instrument Model 49C trace level O_3 analyzer−UV absorption	1-min averages
temp	Rotronic Instrument MP100C thermocouple	1-min averages

site, and that to the north and northwest, including the Upper Peninsula of Michigan and portions of Wisconsin and Minnesota, is largely characterized by relatively flat farmland, forested land, lakes, and populated by small towns and villages. Small cities (populations less than 16 000) near the site include Cheboygan, Petoskey, Traverse City, Alpena, Gaylord, and Grayling. Proximate large urban areas include Detroit, Cleveland, and Toronto, to the south-southeast; Green Bay, Milwaukee, and Chicago, to the southwest; Sault St. Marie to the northeast; and Thunder Bay and Duluth to the northwest. While the site is located near the convergence of Lakes Michigan, Huron, and Superior, it is more than 50 km inland from the nearest shoreline.

Six atmospheric constituents—carbon monoxide, fine particulate matter (diameter between 0.12 and 1.5 μm), coarse particulate matter (diameter greater than 1.5 μm), peroxyacetyl nitrate (PAN), ozone, and isoprene, and one meteorological parameter, temperature—were measured over the period July 29, 1997 to August 17, 1997 and used in this study. Table 1 lists each measured parameter, corresponding measurement technique, and sampling time. Sampling of air for gas measurement was achieved by drawing air through a glass manifold into a small laboratory at the base of the tower. The manifold inlet was 35.2 m above ground level, with an air flow rate of 1646 m per minute, providing for a manifold residence time of less than 1.6 s. The instrument used to detect and size particulate matter was attached to the top platform of the tower, at a height of 31.4 m, with its inlet pointed west, the direction of the most dominate airflow.

To account for the different measurement times, the data matrix **X** was constructed so that each parameter had a value every 5 min. Based on more frequent measurements, 5-min averages were calculated for carbon monoxide, both size fractions of particulate matter, ozone, and temperature, and input directly into the data matrix. Isoprene and PAN both had measurement times greater than 5 min, thus all 5-min intervals between two data points were assumed to have concentrations equal to that of the most recent measurement. Although the data matrix could have averaged the more frequently measured constituents to match the longest averaging time, analysis of such a data matrix revealed that the general structure of results for this study is robust with respect to the length of averaging time. Hence, the aforementioned approach was used to preserve the data signal.

Positive Matrix Factorization. The following section briefly covers the principles of the PMF model. A more thorough discussion of PMF may be found elsewhere (*10*). PMF assumes that a $m \times n$ data matrix **X**, with m constituents of interest and n number of observations, can be factored into the matrixes **F** ($p \times m$) and **G** ($n \times p$) with a residual matrix **E** ($n \times m$).

$$\mathbf{X} = \mathbf{GF} + \mathbf{E} \tag{1}$$

The number of rows in **F**, and the number of columns in **G**, are referred to as the number of factors, p. Each row of **F** represents a single source of pollutants, and the columns of **G** contain the source strength at each observation time. If **G** is dimensionless, with the mean value of each column equal to one, then the elements of **F** are the mean values of each parameter attributed to a particular source.

PMF minimizes Q, the sum of the squares of residuals weighted inversely by the variation of the data points. A nonnegativity constraint is placed on every element in matrixes **F** and **G**.

$$\text{minimize } Q = \sum_{i=1}^{n}\sum_{j=1}^{m} \quad \text{with } F_{ij} \geq 0, \quad G_{kj} \geq 0, \quad k = 1, \ldots, p \tag{2}$$

The value S_{ij} is the standard deviation of X_{ij}. It is desirable to obtain a value of Q equal to the number of elements in **X**, as this represents the situation where the specified standard deviations equal the residuals of the factor analysis. Equation 2 can be solved using an iterative algorithm. A FORTRAN90 program was used for this analysis (*15*). The resulting matrices **F** and **G** do not have to be orthogonal.

The matrix of standard deviations, **S**, was specified in such a way as to indicate the agreement expected between the model and the measured matrix, **X**. Standard deviations were calculated as a fixed fraction, z_j, specific to each parameter, of the observed value, X_{ij}, or the fitted value, Y_{ij}. The advantage of determining error as a percentage of the measured or fitted value is that large values are given large errors, preventing outliers, common in environmental work, from overly influencing factor formation.

During the iterative process of solving eq 2, the matrix **S** was recalculated at each iteration according to eq 3.

$$S_{ij} = z_j \times \max(X_{ij}, Y_{ij}) \tag{3}$$

$$\text{where } \mathbf{Y} = \mathbf{GF}$$

This iterative method of calculating S_{ij} avoids generating error estimates that are too small by taking the larger of the measured matrix and the fitted matrix. Very small standard deviations can lead to apparent matrix singularity or erroneous results. As the standard deviation in PMF is essentially a fitting parameter, values of z_j were determined by knowledge of the relative uncertainty of each constituent's

TABLE 2. Coefficients, z_j, Used to Estimate Standard Deviations

parameter	coeff for estimating SD, z_j
isoprene	0.1
carbon monoxide (CO)	0.05
peroxyacetyl nitrate (PAN)	0.1
particulate matter (PM), coarse	0.1
particulate matter (PM), fine	0.1
ozone	0.05
temp	0.05

measurement and improved by trial and error. Final values for z_j are given in Table 2.

To account for the possible presence of very large outliers which can cause poor results, a robust algorithm was used to solve eq 2. This algorithm increases an error estimate, S_{ij}, according to eqs 4 and 5 if a large outlier is detected.

$$S_{ij,\text{recalculated}} = S_{ij}\sqrt{d} \tag{4}$$

$$d = \frac{E_{ij}}{S_{ij}\alpha} \quad d > 1 \tag{5}$$

The value of α is equal to the outlier distance and was set to 4.0 for this analysis, as recommended by Paatero (*16*). The robust algorithm ensures that a downweighted point exerts the same influence on the fit as a value at the outlier distance from the fitted value.

While Paatero and Tapper (*10*) state that PMF can handle missing data, large blocks of time with missing data for one or more parameters yielded nonmeaningful results in this study. Thus, a subset of the data collected for the seven parameters was selected such that no parameter would have missing data for more than 20 consecutive min. This resulted in a time series with 2116 5-min observation periods. Missing values that did remain in the data matrix were dealt with by inserting the median value of the *j*th column of **X** into the position of the missing data, X_{ij}. This method states that missing data must be similar to the other values in the *j*th column. The standard deviation of a median substituted missing data point was increased by a factor of 50.0 (*16*), causing such points to have a negligible effect on the factors. Measurements below detection limits were given a value equal to one-half of the detection limit for the constituent. Isoprene was the only dataset with measurements below detection during the summer 1997 campaign; less than 10% of its measurements were below detection limits.

Transport Modeling. This investigation utilized the NASA Goddard Space Flight Center isentropic trajectory model. The model has been used for a number of transport studies in the lower and upper atmosphere (*17*−*20*). The model uses global gridded fields of horizontal wind components, temperatures, geopotential heights, and potential vorticity. The gridded wind fields are interpolated spatially to user-selected isentropic surfaces and temporally over time between input fields. Bilinear interpolation of the gridded meteorological data determines winds at parcel locations on the isentropic surfaces. Air parcel advection is calculated using a two-step scheme throughout the trajectory construction. Temperature is interpolated along the parcel path from the gridded data and used with the assumption of potential temperature conservation to compute the parcel pressure at each position. National Meteorological Center gridded (calculated at 2.5° × 2°, 12 standard pressure levels, every 12 h) meteorological data, a time step of 0.05 day, and terminating level of 900 mbar were used for all trajectory calculations. Three-day, backward, boundary-layer trajectories from the field site were calculated every 3 h of the summer campaign. Corresponding trajectories were assigned to each 5-min period of the air quality measurements.

To determine the spatial characteristics of air parcel transport associated with high factor strengths, residence time analysis was used (*21*). A 150 km × 150 km grid was fit to the study domain. With the NASA/GSFC model, trajectory uncertainties grow with transport time; 50−100 km horizontal separation per day of transport (unpublished work) in the lower troposphere. The large grid cells and application of the technique to identification of broad source regions minimizes concern over trajectory calculation errors. The time spent in every grid cell was calculated for all trajectories in a scenario. As all trajectories terminated at the grid cell containing the field site, the transport climatology was corrected for geometry (*22*). Last, the residence probability was determined by dividing the residence time for each grid cell by the total residence time of all cells.

Results and Discussion

Table 3 presents the descriptive statistics of the gaseous species, particulate matter, and meteorological parameters measured at the field site. The atmospheric constituents all experienced large fluctuations over the measurement period with a range of 1−3 orders of magnitude (with the exception of ozone).

A critical step in PMF analysis is determination of the number of factors. One method of choosing the number of factors is to assess the goodness of fit variable, *Q*, defined in eq 2. However, Q was found to decrease smoothly with an increasing number of factors; therefore, no dimensionality was suggested.

It is important to choose the number of factors that provide clear, physically meaningful results while reducing matrix dimensionality as much as possible. The two-factor model did a poor job of explaining isoprene and was not considered a suitable model. Models with greater than four factors were also not considered as they did not reduce the dimensionality of the data matrix significantly. The data were initially analyzed with both three and four factors. However, the four-factor model provided essentially the same factor compositions as did the three-factor model for two of the factors. The remaining two factors of the four-factor model could be added together to obtain the final factor of the three-factor model. Therefore, only the three-factor model will be discussed in the remainder of this work as it provided the greatest reduction in dimensionality, while explaining the underlying structure in the data.

The factor compositions of the three-factor analysis are presented in Figure 2. Explained variation (EV), on the *y*-axis, is a dimensionless number that provides a quantitative statement of how important each factor (source) is in explaining the *j*th column of **X**. The values of EV range from 0 (no explanation) to 1 (complete explanation) and are calculated by eq 6 (*16*).

$$EV(F)_{kj} = \frac{\sum_{i=1}^{n} |G_{ik}F_{ki}|/S_{ij}}{\sum_{i=1}^{n}\left(\sum_{h=1}^{p} |G_{ih}F_{hj}| + |E_{ij}|\right)/S_{ij}} \tag{6}$$

Normalized factor strength time series are plotted in Figure 3. The factor strengths of a particular source are the elements in one column of the matrix **G**.

Factor 1, which explains approximately 87% of the isoprene data, is clearly evident as a single source in Figure 2a. In many cases the appearance of such a factor must be

TABLE 3. Descriptive Statistics of Each Measured Parameter

measurement	units	*N*	mean	SD	median	range
isoprene	ppb	2099	1.136	1.402	0.447	0.007−7.296
carbon monoxide (CO)	ppb	1918	107.6	41.5	101.7	19.6−227.2
peroxyacetyl nitrate (PAN)	ppt	2029	235	203	163	23−867
particulate matter (PM), coarse (diameter > 1.5 μm)	number/cm^3	2116	0.447	3.623	0.116	0.010−64.254
particulate matter (PM), fine (0.12 μm < diameter < 1.5 μm)	number/cm^3	2116	705.0	658.9	379.1	81.8−2399
ozone	ppb	2095	35.9	16.8	30.8	12.4−83.2
temp	°C	2073	22.3	4.1	22.0	14.1−32.3

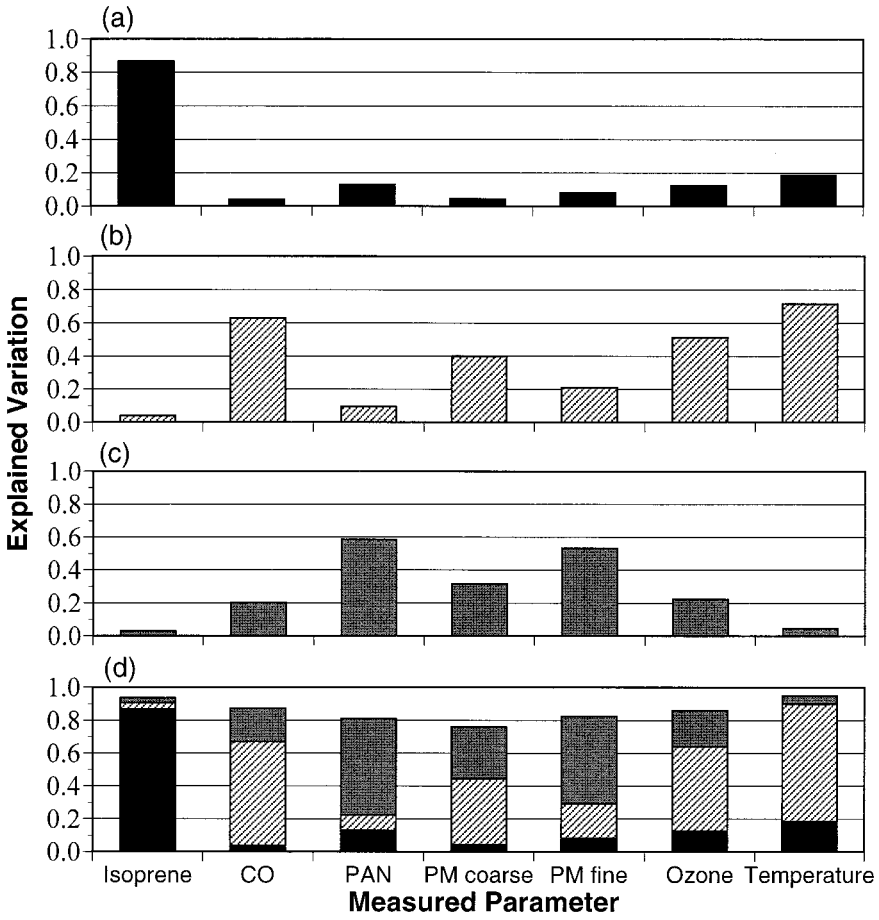

FIGURE 2. Variance of the measured parameters explained by each of the three sources in the three-factor PMF model: (a) factor 1—isoprene-dominated, (b) factor 2—local source, (c) factor 3—long-range transport, and (d) cumulative variance explained by the PMF analysis.

viewed with suspicion as it may simply be the result of specifying too small of error estimates for one species. However, the time behavior of isoprene is strongly diurnal, with relatively high values during mid-day and very low values at night, a behavior much different than that of the other measured constituents. While other parameters have a diurnal signal due to micrometeorological cycling, none have as great a magnitude as isoprene production. Thus, the isoprene data tends to obtain its own factor. The corresponding factor strength time series (Figure 3a) has a diurnal behavior similar to the measured isoprene concentrations. As a result of these findings, factor 1 is classified as an isoprene-dominated source.

As compared to the other two factors, the second factor identified (Figure 2b) best explains temperature (72%), carbon monoxide (63%), and ozone (52%). This factor also describes 40% of the variation in coarse particulate matter. The factor strength time series (Figure 3b) shows a relatively compressed signal, with less variation about its mean than the other factors, indicative of local air pollution at a rural site. Carbon monoxide is emitted locally by traffic along Interstate-75 and other nearby roads, the Pellston airport, and the light industry and residential areas located in northern Michigan. These local emissions also have the ability to produce relatively low mixing ratios of ozone. Coarse particulate matter is most likely due to local emissions as larger particles have brief atmospheric residence times due to deposition.

From a spectral density analysis of this time series, a slight diurnal signal is revealed—higher factor strengths during the night and lower factor strengths during the day, indicating that this signal is partly influenced by the diurnal pattern in boundary layer height. This pattern is observed regardless of transport direction, confirming the absence of land-lake influences. Temperature is probably incorporated in this source as it has a diurnal signal that correlates with the rising and falling of the boundary layer. General tendencies are for temperatures to be warmer and the boundary layer thicker during the day, with the opposite situation at night. It is also to be expected that locally produced ozone would be

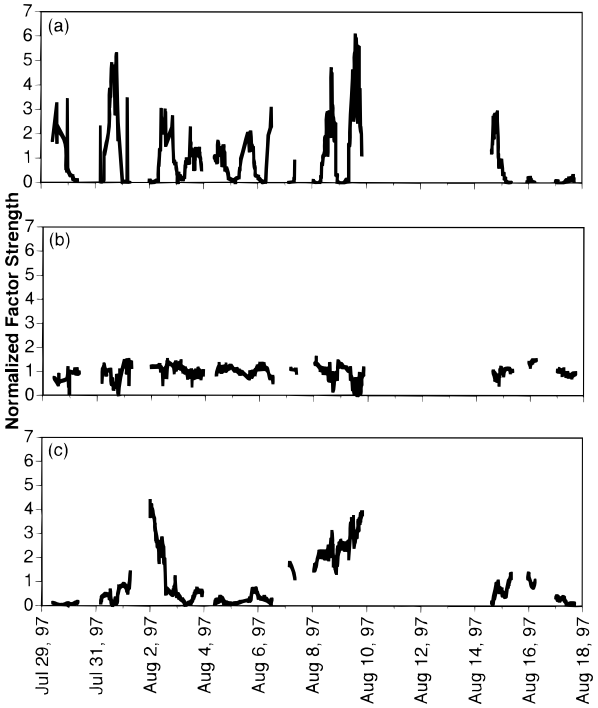

FIGURE 3. Normalized factor strength time series: (a) factor 1—isoprene-dominated, (b) factor 2—local source, and (c) factor 3—long-range transport.

correlated with temperature. Factor 2 is therefore identified as a local source.

The third source determined by the PMF analysis explains almost 60% of the variance in PAN, 53% of the fine and 31% of the coarse particulate matter variance, and approximately 20% of the variance in carbon monoxide and ozone. This factor exhibits lower frequency variations with clear pollution episodes on August 1−3 and August 7−10. The factor strength time series suggests a long-range transport source, as does the fact that PAN, a well-aged NO_Y species, is well explained by this factor. Fine particulate matter, due to its low terminal velocity, can be transported great distances, and, with a cutoff of 1.5 μm, it is possible that some of the particulate matter classified as coarse could also be transported a substantial distance before falling out. Carbon monoxide, a slowly reactive compound, and ozone transport are expected from urban areas as well. The variability in factor 3 is similar in periodicity to that of air mass changes due to synoptic climatology. Factor 3 is thus referred to as a long-range transport source.

From Figure 2d, it is evident that the use of three factors explains over 90% of the variation in isoprene and temperature. Over 80% of the variation in carbon monoxide, fine particulate matter, PAN, and ozone and nearly 75% of the variation in coarse particulate matter are explained.

To further ascertain the nature of each of the three sources, PMF source strength was paired with corresponding wind direction measurements (R. M. Young wind vane) taken at the top of the tower. Figure 4 shows the results of plotting factor strength versus wind direction. There is a greater density of data points in the western quadrants as winds at the site typically were from the west. Accordingly, the isoprene-dominated source is skewed toward flow from this direction (Figure 4a). The relatively high factor strengths of Factor 1 associated with flow from the south are attributed to the corresponding warmer air temperatures. Studies of isoprene emissions have shown a positive correlation with leaf temperature and isoprene emissions (*23*). For the local source, factor strength is independent of wind direction (Figure 4b). The long-range transport source has a strong southwestern lobe (Figures 4c) consistent with the transport of pollutants from the industrial and urban areas southwest of the site (Figure 1).

To examine the characteristics of factor 3, the long-range source, residence time analysis was performed. Residence time probabilities for air arriving at the field site during times when factor 3 strength was greater than its mean are mapped in Figure 5. Air transport represented by these trajectories traveled 1450 km over 3 days, on average. Air arriving when factor 3 is strongest spends most of its time over western Michigan and the southern Lake Michigan coastal areas in Wisconsin, Illinois, and Indiana. The weaker northwesterly lobe results from greater PAN transport in the colder descending air, as assessed by daily long-range trajectory analysis. Summing the individual cell probabilities reveals that nearly 65% of the long-range source areas resulting in high factor 3 strength reside in the southwest quadrant from the site.

One of the strengths of PMF is that the contribution each factor makes to a particular species can be easily determined in the units the species was originally measured. If the matrix **G** is normalized, then the matrix **F** contains the mean values of each parameter attributed to a particular source. Table 4 lists the mean values contributed by the three factors to each measured species. Adding these contributions up for each species yielded the sum of the factor contributions, which was then compared to the mean of its measurements. The three-factor PMF model did a good job of recreating the measured mean for all parameters except for coarse particulate matter. The poor results for coarse particulate matter may be due to the fact that although concentrations were generally less than 1 particle/cm^3 for the 3 weeks of measurements, a brief spike in concentration occurred between 6 and 7 a.m. on August 6, with concentrations as high as 64 particles/cm^3. No similar spike was observed in any of the other measured parameters.

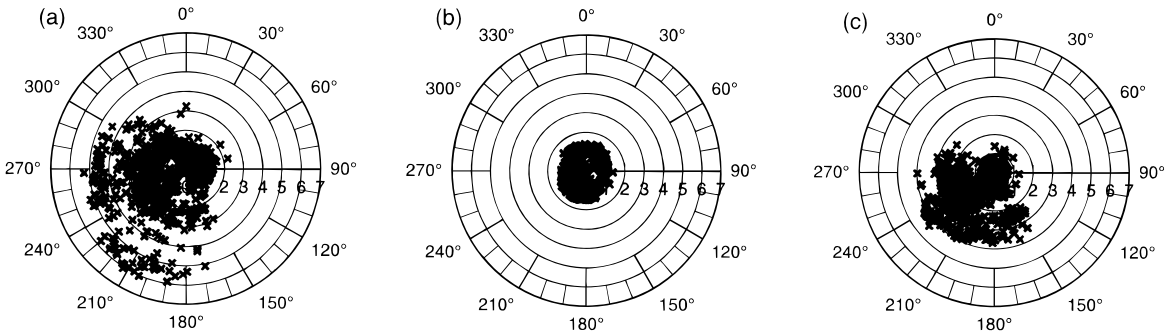

FIGURE 4. Factor strength plotted as a function of wind direction: (a) factor 1—isoprene-dominated, (b) factor 2—local source, and (c) factor 3—long-range transport.

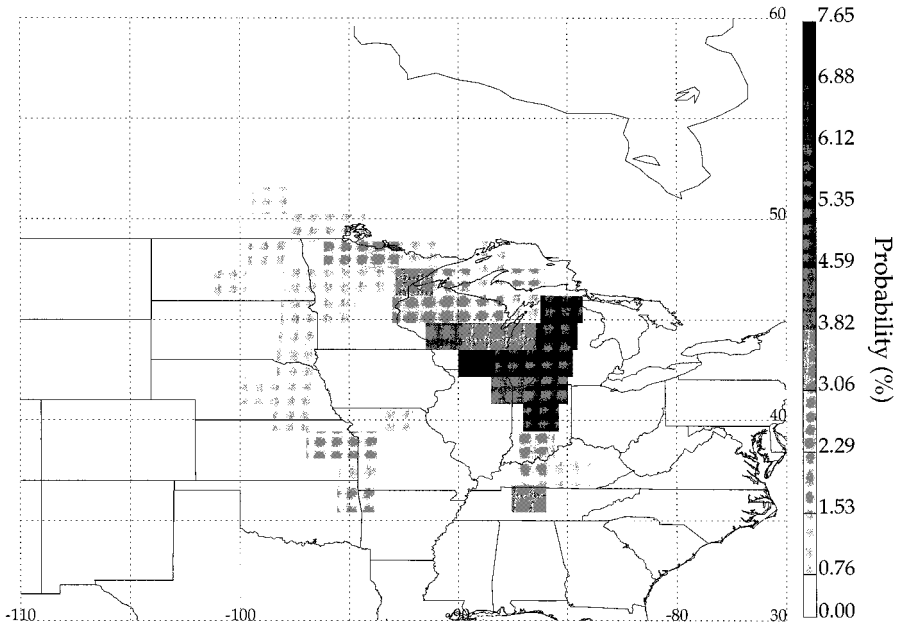

FIGURE 5. Residence time map for those times when factor 3, long-range transport, strength was greater than its mean value. Darker grid cells indicate a higher probability of air parcel residence over that area. The total probability of residence over all the colored areas equals 100%.

TABLE 4. Mean Values Contributed by Each Factor to the Measured Species

	isoprene (ppb)	CO (ppb)	PAN (ppt)	PM coarse (number/cm^3)	PM fine (number/cm^3)	ozone (ppb)	temp (°C)
factor 1—isoprene-dominated	1.128	4.0	25	0.006	43.2	5.4	5.0
factor 2—local source	0.003	71.0	11	0.053	87.7	18.2	16.0
factor 3—long-range transport	0.002	29.4	174	0.067	499.8	11.4	1.2
sum of factor contributions	1.132	104.4	210	0.126	630.7	35.1	22.2
measured mean	1.136	107.6	234	0.447	704.99	35.9	22.3
% difference	−0.3	−3.0	−10.4	−71.8	−10.5	−2.1	−0.5

In summary of the work described herein, air quality data collected during the summer of 1997 near Pellston, MI as a part of the PROPHET measurement initiative, was subjected to a relatively new method of factor analysis, positive matrix factorization. PMF was found to provide physically interpretative nonnegative factors that utilized the error estimates of the data. Three factors were identified: an isoprene-dominated source, a local source, and a long-range transport source. The factor strength of the local source had the least variability about its mean, while the factor strength of the isoprene-dominated source has the greatest variability about its mean. Southwesterly winds were common during the times of relatively high factor strengths for the long-range transport source, indicating transport of fresh pollution from the industrial Midwest. The average contribution by each factor (in units of mixing ratio, number concentration, and degrees) was determined for each measured parameter, enabling the modeled matrix to be compared to the data matrix. Good agreement between the fitted and data matrix was achieved for all parameters with the exception of coarse particulate matter.

The methodology reported herein provides an analytical framework for source attribution and apportionment that could be readily adapted to other measurement sites. Future work includes a comparison of PMF to the more traditional method of receptor analysis, principal component analysis.

Acknowledgments

The authors would like to thank the staff at the University of Michigan Biological Station. Funding provided by the National Science Foundation and Michigan Technological University Department of Civil and Environmental Engineering for this work is also gratefully appreciated. This research is part of PROPHET, Program for Research on Oxidants: PHotochemistry, Emissions and Transport—a consortium of scientists from university, government and private industry to improve the scientific understanding of the sources, sinks, and impacts of photochemical oxidants.

Literature Cited

(1) Watson, J. G. *J. Air Pollut. Control Assoc.* **1984**, *34*, 619−623.
(2) Jackson, J. E. *A User's Guide to Principal Components*; John Wiley & Sons: New York, 1991.
(3) Poissant, L.; Bottenheim, J. W.; Roussel P.; Reid N. W.; Niki, H. *Atmos. Environ.* **1996**, *30*, 2133-2144.
(4) Wolff, G. T.; Korsog, P. E.; Kelly, N. A.; Ferman M. A. *Atmos. Environ.* **1985**, *19*, 1341−1349.
(5) Pio, C. A.; Nunes, T. V.; Borrego, C. S.; Martins, J. G. *Sci. Total Environ.* **1989**, *80*, 279−292.
(6) Wolff, G. T.; Morrissey, M. L.; Kelly, N. A. *J. Climate Appl. Meteorol.* **1984**, *23*, 1333−1341.
(7) Baek, S.; Choi, J.; Hwang, S. *Environ. Int.* **1997**, *23*, 205−213.
(8) Pio, C. A.; Castro, L. M.; Cerqueira, M. A., Santos, I. M.; Belchior, F.; Salgueiro, M. L. *Atmos. Environ.* **1996**, *30*, 3309−3320.
(9) Henry R. C.; Hidy, G. M. *Atmos. Environ.* **1982**, *16*, 929−943.
(10) Paatero, P.; Tapper, U. *Environmetrics* **1994**, *5*, 111−126.
(11) Juntto, S.; Paatero, P. *Environmetrics* **1994**, *5*, 127−144.
(12) Anttila, P.; Paatero, P.; Tapper, U.; Järvinen, O. *Atmos. Environ.* **1995**, *14*, 1705−1718.
(13) Starn, T. K.; Shepson, P. B.; Bertman, S. B.; White, J. S.; Splawn, B. G.; Riemer, D. D.; Zika, R. G.; Olszyna, K. *J. Geophys. Res.* **1998**, *103*, 22 425−22 435.

(14) Nouaime, G.; Bertman, S. B.; Seaver, C.; Elyea, D.; Huang, H.; Shepson, P. B.; Starn, T. K.; Riemer, D. D.; Zika, R. G.; Olszyna, K. *J. Geophys. Res.* **1998**, *103*, 22,463−22,471.
(15) Paatero, P. *Chemom. Intell. Lab. Syst.* **1997**, *37*, 23−35.
(16) Paatero, P. *User's Guide for Positive Matrix Factorization Programs PMF2.EXE and PMF3.EXE*; University of Helsinki: Finland, 1996.
(17) Schoeberl, M. R.; Lait, L. R.; Newman, P. A.; Rosenfield, J. E. *J. Geophys. Res.* **1992**, *97*, 7859−7882.
(18) Schoeberl, M. R.; Lait, L. R.; Newman, P. A.; Krueger, A. J. *J. Geophys. Res.* **1993**, *98*, 2949−2956.
(19) Pickering, K. E.; Thompson, A. M.; McNamara, D. P.; Schoeberl, M. R. *Mon. Wea. Rev.* **1994**, *122*, 864−879.
(20) Pickering, K. E.; Thompson, A. M.; McNamara, D. P.; Schoeberl, M. R.; Fuelberg, H. E.; Loring Jr., R. O.; Watson, M. V.; Fakhruzzaman, K.; Bachmeier, A. S. *J. Geophys. Res.* **1996**, *101*, 23 909−23 925.
(21) Poirot, R. L.; Wishinksi, P. R. *Atmos. Environ.* **1986**, *20*, 1457−1469.
(22) Paterson, K. G.; Honrath, R. E.; Subhash, S. S.; Sweet, C. I. *Proceedings: Atmospheric Deposition Conference, VIP-72, A&WMA*; 1997, pp 192−211.
(23) Lamb, B.; Westberg, H.; Allwine G. *J. Geophys. Res.* **1985**, *90*, 2380−2390.

Received for review June 15, 1998. Revised manuscript received November 10, 1998. Accepted November 24, 1998.

ES980605J